Signatures of Nonlinear Compton Scattering in Scattered Angular Spectra

Brandon K. Russell,[1, a)] Stepan S. Bulanov,[2] Qian Qian,[1] Sergey V. Bulanov,[3] Gabriele Grittani,[3] Daniel Seipt,[4] Christopher Arran,[5] Christopher P. Ridgers,[5] Thomas Blackburn,[6] Stuart P. D. Mangles,[7] and Alexander G. R. Thomas[1]

[1)] *Gérard Mourou Center for Ultrafast Optical Science, University of Michigan, 2200 Bonisteel Boulevard, Ann Arbor, Michigan 48109, USA*

[2)] *Lawrence Berkeley National Laboratory, Berkeley, California 94720, USA*

[3)] *ELI Beamlines Facility, The Extreme Light Infrastructure ERIC, Za Radnicí 835, Dolní Břežany, 25241, Czech Republic*

[4)] *Helmholtz Institute Jena, Fröbelstieg 3, 07743 Jena, Germany*

[5)] *Department of Physics, York Plasma Institute, University of York, York YO10 5DD, United Kingdom*

[6)] *Department of Physics, University of Gothenburg, SE-41296 Gothenburg, Sweden*

[7)] *The John Adams Institute for Accelerator Science, Imperial College London, London, SW7 2AZ, UK*

(Dated: 19 November 2024)

In this paper we want to find experimentally measurable signatures that can differ between models of Compton Scattering, i.e., classical vs. quantum, and LCFA vs. LCFA colinear vs. LMA. Scans will be performed over laser and electron beam parameters in a colliding beam geometry, e.g. divergence, energy spread, beam radius, mean energy, a_0. These scans will performed with the different models to determine what the main signatures are. These signatures will be sent to realistic detectors to determine whether they are experimentally measurable. This should give the minimum parameters that the next-generation of laser facilities will need to obtain to properly measure nonlinear Compton. The work will be done using the particle tracking code Ptarmigan which has been modified to include colinear emission and the ability to read in raw data from PIC codes and experiments to obtain realistic results.

I. INTRODUCTION

There are currently a new set of ultra-intense lasers coming online that will push to intensities $> 10^{23}$ W/cm^2 with the primary goal of studying strong field quantum electrodynamic (SFQED) processes. Specifically, the processes of interest are non-linear Compton scattering (NLCS) and non-linear Breit-Wheeler (NLBW) pair creation. These processes are expected to occur in the most energetic environments in our universe, such as those around extremely strongly magnetized neutron stars known as magnetars. The theoretical models for NLCS and NLBW are fundamental to the modeling efforts in the field of extreme astrophysics and future ultra-intense laser experiments, therefore experimental validation of these models is important. While the linear versions of these quantum electrodynamic theories are well tested, only a few preliminary experiments have been performed to validate the nonlinear counterparts, however these experiments did not have sufficient statistics and clear enough signatures to inform the models.

The current NLCS experiments have largely struggled due to the low probability of this process occurring at currently available laser intensities. In NLCS, several photons scatter from a single particle to produce a single high energy photon, i.e., $e^- + n\gamma \rightarrow e^- + \gamma'$. The probability of NICS occurring in the interaction of electrons with laser that have intensities that can currently be reached is extremely low. The probability depends on the parameter $\eta = |F^{\mu\nu} p_\nu|/mE_s$, where $F^{\mu\nu}$ is the field tensor, p_ν is the particle 4-momentum and $E_s \approx 1.3 \times 10^{18}$ V/m is the Schwinger field. As η approaches unity NLCS becomes much more probable, however reaching this regime in the interaction of a laser pulse with an electron at rest requires a laser intensity $I \approx 10^{29}$ W/cm^2. Instead, if a laser pulse collides head-on with a relativistic electron beam the laser electric field in the boosted frame will be $\sim 2\gamma$ larger than the lab frame, where γ is the Lorentz factor, greatly reducing the intensity requirement.

These head-on experiments have focused on finding signatures of radiation reaction (the change in momentum a particle experiences when it emits a photon) in the electron and photon energy spectra. Classical radiation reaction (CRR) predicts a higher emission rate than quantum radiation reaction (QRR) and can predict a nonphysical photon spectra where photon energies exceed the energy of the electrons. These differences manifest themselves in different predicted shifts in the electron spectra. However, if η is small then these shifts will not be significant enough to be measurable. In addition to measuring differences between CRR and QRR, it is also important to validate the models used for NLCS, in particular the local constant field approximation (LCFA) and the local monochromatic approximation (LMA). LCFA is the main model used in the popular particle-in-cell codes, allowing for NLCS to be simulated in plasmas. LCFA and LMA predict similar photon spectra at high energies however, below keV energies the models diverge as

[a)] Electronic mail: bkruss@umich.edu

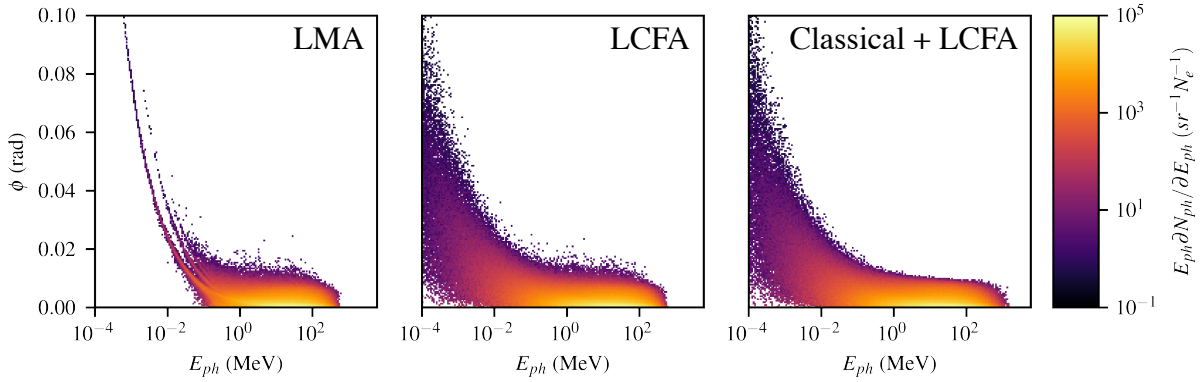

FIG. 1: Characteristic NLCS photon angular spectra generated in Ptarmigan using the LMA, LCFA, and LCFA + classical radiation models. These spectra were generated in the head-on collision of a collimated 1 GeV mono-energetic electron beam with a 25 fs FWHM duration laser with a normalized vector potential $a_0 = 15$.

LCFA greatly over predicts the photon number. Measuring these differences in the energy spectra is non-trivial in experiments and so far have not been measured.

A potential path to finding signatures that may more easily differentiate between the RR and NLCS models is to look a the angular spectra of both the photons and electrons. This is not something that can be generally considered because particle in cell codes have generally made the co-linear emission approximation, where photons are emitted directly along the path of particle propagation. While this approximation is generally true for high energy photons because the cone of emission goes as $1/\gamma_e$, it is not accurate for the low energy photons. In this manuscript the signatures of the different models of RR that manifest in the angular spectrum will be identified and explored under various experimental conditions. This will be done over a large parameter range, taking into account the error associate with real measurement techniques, thereby allowing us to define the minimum laser and electron beam parameters necessary to measure differences in the RR models.

II. METHODS

To perform this study the Monte Carlo code Ptarmigan was chosen. This code was chosen due to the implementation of multiple radiation models (classical, LMA, LCFA) which all include angular emission. The details of the Ptarmigan implementation have been outlined by Blackburn *et al.*[1]. An electron distribution with a Gaussian temporal and spatial profile was populated through rejection sampling using N particles. The beam had an energy spread σ_E, length L_e, mean Lorentz factor $\langle\gamma_e\rangle$, radius r_e, and RMS divergence σ_d. The electron beam was set to propagate head-on into a Gaussian laser pulse. This laser pulse had a normalized vector potential a_0, wavelength λ, waist w_L, FWHM duration τ_{FWHM}, and was either linear or circularly polarized.

Electrons are individually sent through the laser pulse, therefore the self-fields of the beam are not taken into account. The motion of particles is calculated by the relativistic Lorentz force equation if LMA or LCFA are used and the Landau-Lifshitz equation of motion if the classical solver is used. During the propagation of the particle through the laser fields on each timestep the probability of photons being generated is checked. If a photon is generated, the angle and energy of the photon calculated pseudo-randomly based on rate tables for LCFA, LMA, or classical. If radiation reaction is turned on, the emitting particle will receive a momentum kick due to photon emission. Additionally, the momentum from the absorption of photons from the background is taken into account, however laser depletion is not included. We modified the code to also allow for co-linear photon emission, allowing for comparison with PIC code results. Photons that are generated will also propagate through the laser fields and will randomly generate electron-positron pairs based on NBW rates. These generated particles will also propagate through the fields, allowing for the generation of pair-cascades.

III. IDENTIFYING SIGNATURES

Fig. 1 shows the photon angular spectra for three different radiation models, LMA, LCFA and LCFA + classical. In previous works, only the angularly integrated spectra have been analyzed, which only allow for a few signatures to be found that differentiate between the NLCS models. Specifically these are, the higher peak photon energy from classical, and the larger number of low energy photons predicted by LCFA compared to LMA. However, by looking at the angular spectra we can observe a few primary differences. Firstly, for a particular energy QRR using either LCFA or LMA will predict photons out to larger ϕ, to angles that are not allowed by CRR. Secondly, LMA predicts photons at larger ϕ than LCFA for energies $E_{ph} <$ MeV. Finally, LMA predicts harmonics that appear as multiple curves in the angular

spectra. In the following sections we will consider these three signatures in detail.

A. Harmonics

The harmonics in LMA come from the scattering of s background photons and can be shown analytically through energy-momentum conservation which is written as follows:

$$q + sk = q' + k'. \tag{1}$$

Here, $q = p + (a_0 m^2/2kp)$ and q' are the quasi-momentum of the electron before and after scattering, with an initial 4-momentum p. This electron scatters s background photons with a 4-momentum k into a photon with 4-momentum k'. By squaring Eqn. 1 and removing q' by plugging Eqn. 1 into the squared equation, we can solve for the angle dependent photon frequency. Specifically for the case of a head-on collision the solution is:

$$\nu'(\phi) = \frac{s\nu\gamma(1+\beta)}{\gamma(1+\beta\cos\phi) + (s + \frac{a_0^2}{2\nu\gamma(1+\beta)})\nu(1-\cos\phi)}. \tag{2}$$

Here $\beta = v/c$, and $\nu = \hbar\omega/mc^2$ is the normalized frequency. At a particular ϕ the energy of the scattered photon will increase with the number of background photons scattered, however the energy change between harmonics decreases with increasing harmonic order.

For the collision of a monoenergetic 1 GeV beam with an $a_0 = 15$ pulse shown in Fig. 1, clear separations are observed in the 1 - 100 keV range. In this range, photons can be measured directly onto an x-ray camera, or onto a scintillator that is imaged by a camera. If a camera were to image the photons off-axis and resolve the photon spectrum, a multi-peaked spectrum should be measured. However, this assumes that the peaks in the spectrum can be resolved and that the peaks will not merge together under realistic experimental conditions. Additionally, the signal of each peak will be lower than the previous order, because the scattering probability decreases with increasing harmonic order.

To study the harmonics under realistic experimental conditions we performed several parameter scans of a_0, beam divergence, beam energy, and energy spread. Fig. 2 shows several sample spectra from these scans to demonstrate the trends. As a_0 is increased, the width of the harmonic lines increases and the number of photons scattered to larger angles and into higher harmonics increases. This is expected due to the a_0 dependence in Eqn. 1, showing a decrease in scattered photon energy with increased a_0. The contribution to the width of the harmonic lines due to a_0 can be approximated by taking the difference between Eqn. 2 when $a = 0$ and when $a = a_0$. Additionally, the change in energy between two harmonics for a particular ϕ, taking into account a_0 can be estimated by taking the difference between Eqn. 1 substituting $s \to s+1$ and $a = a_0$, and Eqn. 1 with $a = 0$. To estimate the lower limit where the harmonics become separate and therefore potentially measurable, we can set this equation equal to 0, to get:

$$\phi_{cross}(s, a_0, \beta) = \cos^{-1}\left(\frac{2 - sa_0^2(1-\beta)}{sa_0^2(1-\beta) + 2\beta}\right). \tag{3}$$

If a_0 is small, then the s and $s+1$ harmonic lines will not cross and ϕ_{cross} will be imaginary. This does not account for the complete width of the lines because multiple scattering causes a reduction in γ and therefore an increase in line width. However, using this equation we can estimate the minimum angle that a detector can be placed at to observe separate harmonics.

The scan of γ shows a particularly interesting result. As γ decreases more harmonics appear at larger angles, potentially making the measurement of these harmonics possible. However, reducing γ also reduces the energy at which the harmonic lines are separated. A balance must then be met between having a small enough γ such that the photon are not along the beam propagation axis, but large enough that the harmonics form at energies that are detectable by a chosen detector. Additionally, a large a_0 is necessary such that there is a significant probability of photons being scattered into the harmonic lines. In plasma physics we generally view a_0 as a measure of how relativistic an interaction is, however a_0 also defines how many photons a single electron will interact with. This point was discussed in the work of Seipt *et al.*[2], where they derive the equation for the most probable number of photons absorbed by an electron i.e., the most probable harmonic. This equation is:

$$\langle s \rangle_e = 0.54 \frac{a_0^3}{1 + 1.49\chi_e^{0.59}}, \tag{4}$$

where $\chi_e = 2\gamma_e a_0 \omega/m$. From this equation we see that the most probable harmonic increases with a_0 and decreases with γ consistent with our simulations.

For measuring the harmonics we must also consider how energy spread and divergence will affect the harmonic lines. As seen in Fig. 2 both of these properties act to broaden the harmonics, however they appear in different ways. Divergence broadens the lines, causing all the harmonics to merge into a single line for divergences exceeding a few mrad. Energy spread appears to form a background of photons between the lines, however even at largest energy spread in our scan (40%) the lines can still be distinguished. From our scans it seems that divergence angles less than a few mrad and energy spreads less than 10% are necessary to form distinct harmonic lines.

Now that we have established how the harmonics vary with beam and laser properties we can consider how they might be detected. The harmonics form in the 1-100 keV range which is the same range betatron radiation falls into. This complicates the measurement because betatron radiation will be formed if the electron beam used is

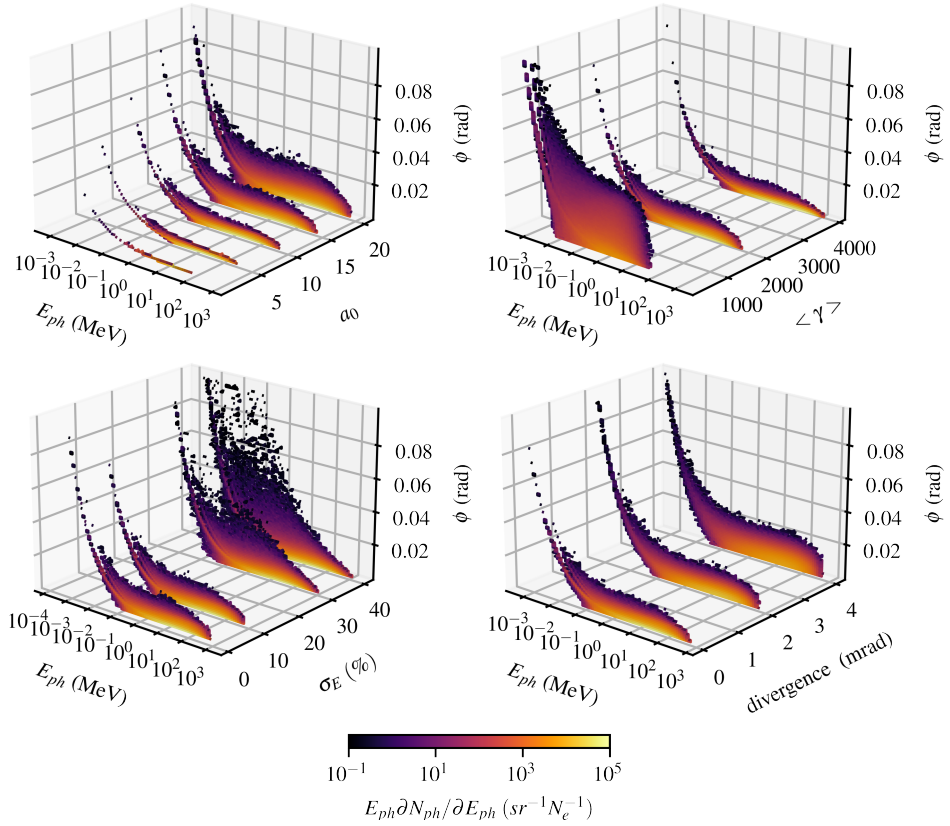

FIG. 2: Scans of a_0, γ, divergence angle, and energy spread σ_E. The base simulation is a monoenergetic 1 GeV beam interacting with a 27 fs, $a_0 = 15$ linear polarized laser.

accelerated by wakefield acceleration. If the beam comes from a conventional linear accelerator this will not be a problem. The benefit of betatron exisiting in this range is that there has already been some effort to develop diagnostics. Albert *et al.* used a stack of image plates to obtain angular spectra of the photons in the keV range[3]. However, the analysis technique requires an assumption on the shape of the spectra and is therefore not applicable to the measurement of harmonics where we are attempting to directly measure the spectral shape. Another method is to diffract the scattered photons from a crystal. This measurement allows for a very narrow range of photon energies to be measured with high resolution. Although this could be quite a good technique for measuring single spectral lines, it is not ideal if we want to fully resolve the harmonics. The best option may be to use single photon counting to construct the spectrum. This method was used by Behm *et al.* to measure differences in betatron spectra transmitted through thin Al foils[4].

For the single photon counting method we consider placing a detector somewhere off the collision axis such that it collects only part of the scattered photons. From the simulations we can create synthetic data to assess the viability of this method. The synthetic detector is created by placing a plane at some position and mapping the position of all photons incident on the plane. A 2D histogram is then created where the size and number of bins is based on a particular x-ray CCD. We have assumed the same CCD as used by Behm *et al.*, the Andor iKon-M which which has a 13.3×13.3 mm^2 detector with 1024×1024 pixels. The result of this is shown in Fig. 3. A linear response has been assumed for the detector i.e., the CCD counts of a pixel are linearly proportional to the energy of the incident photon. This is also approximately true for real detectors, however there will also be diffusion of charge from pixels into other pixels and quantum noise that will result in error on the pixel value. The main requirement of this method is to have few photons incident in a single shot such that multiple photons do not hit the same pixel, however enough photons such that the spectrum can be resolved. To reduce the photon density the detector can simply be moved away from the interaction. This will reduce the signal which can be solved by integrating multiple shots. For Fig. 3 the detector has been placed at and angle and at a distance from the interaction where the separation between the harmonics can be resolved. In an experiment it is the separation between the lines that is important to measure. The LCFA does not predict the absence of photons in these regions, instead it predicts a smooth spectrum.

An experiment that implements this single photon

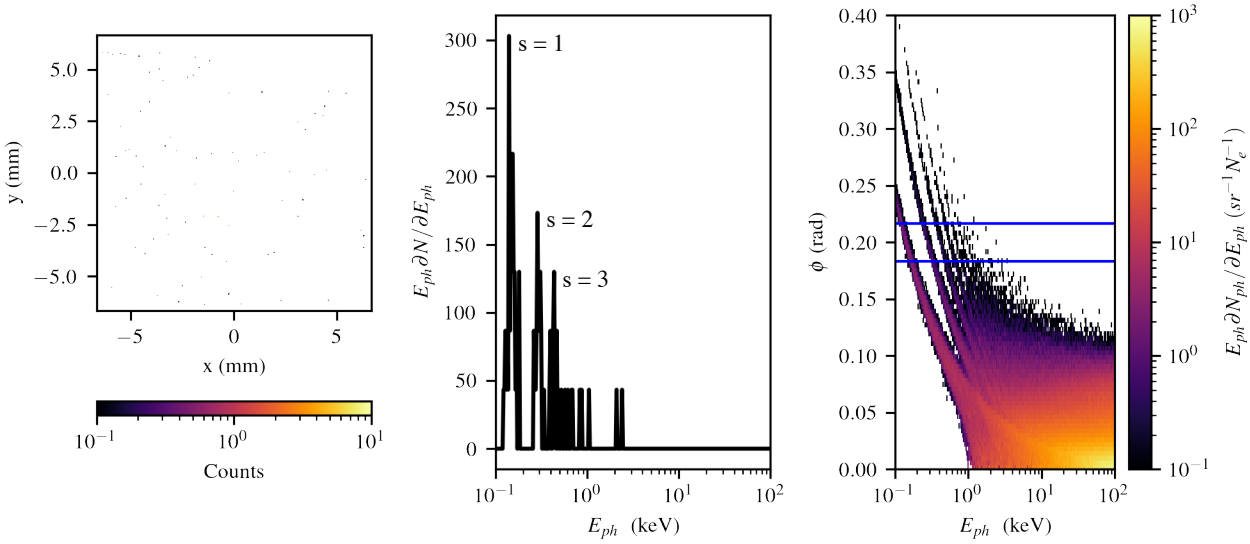

FIG. 3: Synthetic detector demonstrating measurement of harmonics through single photon counting. The detector is modeled based on the Andor Ikon-M with 1024×1024 pixels placed 40 cm and 0.2 rad from the collision axis.

counting technique to differentiate between the LCFA and the LMA would need to prove with sufficient statistics that the keV part of the scattered spectrum is modulated. Due to shot-to-shot fluctuations, ideally the spectrum would be sufficiently resolved on a single shot. Accumulating over several shots is possible, however it will result in a blurring of the spectral lines as the angle of the beam changes. This can be achieved by placing the detector close enough to the interaction that there is a large flux of photons, but not too close that there are a significant number of multiple hits on the pixels. Additionally, by moving the detector closer, the range of angles captures by the detector, and because the harmonic lines are not vertical (Fig. 3) this will increase the linewidth in the angularly integrated spectrum. This set of opposing factors leads to an optimization problem for the detector position. Experimentally, the position of the detector can be scanned to obtain sufficent statistics and separation between harmonics.

B. Classical RR vs. Quantum RR ϕ_{max} edge

The next signature that we can consider is the hard edge in the radiated photon spectra that forms in CRR, but does not form in QRR. This edge forms as classically radiation is produced as a spectrum, not the quantized scattering of incoming photons. The conservation of momentum and energy is therefore different for classical RR as it is just an electron oscillating in the electric fields, producing a synchrotron-like spectrum. We know that the classical description cannot be correct because it allows for the production of photons with energies exceeding the energy of the incoming electron. This can be seen in Fig. 4 where classical LCFA overpredicts the

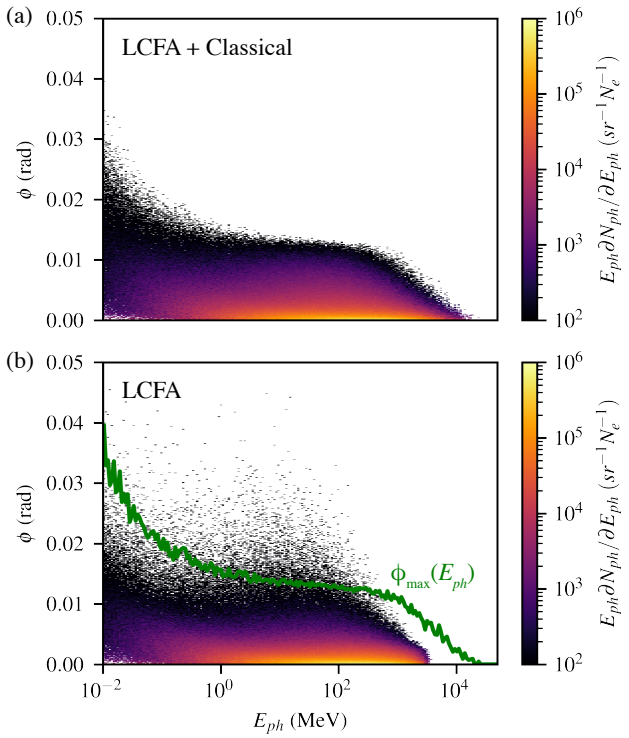

FIG. 4: Classical and quantum photon angular spectra. A line was fit to the classical ϕ_{max} edge and plotted on over the quantum spectrum to demonstrate the existence of photons above this edge. Simulation uses $\gamma = 7814$, $a_0 = 25$.

maximum photon energy. However, it is not simple to experimentally discriminate between CRR and QRR from the difference in the predicted photon spectra and the

resulting difference in the electron spectra. Indeed, this was attempted in the work of Cole *et al.*[5], while the data clearly showed evidence of radiation reaction, it was insufficient to determine the radiation model. Perhaps the angular spectra may allow us to discriminate between the models.

To study this we first fit a line to the classical edge to generate the line $\phi_{max}(E_{ph})$. This is shown in Fig. 4 plotted over the quantum spectrum. Note that classically photons cannot exist at larger angles than this line, however QRR predicts many photons outside of this line, particularly in the 1-100 MeV range. Due to the energy of these photons we cannot use the same single photon counting method that we proposed to measure the harmonics. Instead, this range requires the use of scintillators, perhaps CsI or LISO. Arrays of CsI crystals have already been used to measure non-linear Compton spectra[5]. This type of detector was reported by Behm *et al.* as a way to resolve spectra in the MeV range[6]. Measuring spectra with this detector is non-trivial and requires prior knowledge of spectral shape. We can envision placing this detector at a specific scattering angle such that it captures photons only above the classical edge. If photons are detected with a spectral shape and number that is consistent with QRR, then this can be used to discriminate between the radiation models. For this measurement to be possible the number of photons above the classical edge must be sufficient be be detectable above the background. The MeV range of photons exist and very small scattering angles, therefore electrons which will may scintillate should be deflected away.

To understand what beam and laser parameters are necessary to measure the classical edge we again performed several simulations scanning these properties. The results of these scans are shown in Fig. 5. The important quantity that we focused on in the scans is the number of photons above the classical edge. The photons above the line $\phi_{max}(E)$ that was fit to the classical simulation for energies > 0.1 MeV was integrated and normalized to the total number of photons in the quantum simulation. Fig. 5(a) shows this quantity varying a_0 and $\langle\gamma\rangle$. At low a_0 and $\langle\gamma\rangle$ increasing these parameters results in a larger number of photons above the classical edge. However, percentage of photons peaks when $\chi \approx 0.6$ and falls off for larger χ. For small a_0, the classical and quantum spectra appear to be very similar, with the main difference appearing as the shift in the peak energy of the spectrum. Very few photons are observed outside the classical ϕ_{max} line. As $\langle\gamma\rangle$ and a_0 increase towards the peak at $\chi = 0.6$, the angle of the classical edge decreases. The photons in the quantum spectrum also appear closer to the propagation axis, however the number of photons above the classical edge greatly increases. As $\langle\gamma\rangle$ and a_0 further increase, a very low photon number tail forms that more than doubles the maximum scattering angle in the MeV range from ~ 8 mrad to > 20 mrad. Although QRR predicts an even longer tail in the angular spectra, the photon number in this tail is very small, resulting in the dependence seen in Fig. 5.

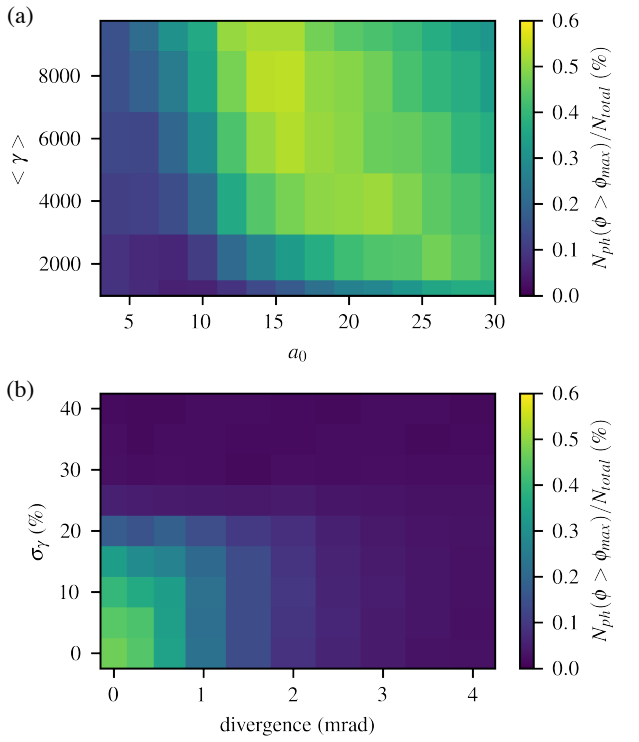

FIG. 5: Percentage of photons above the classical ϕ_{max} for the range of photon energies shown in Fig. 4. In (a) a_0 and $\langle\gamma\rangle$ are varied for a collimated monoenergetic beam. In (b) divergence and energy spread are scanned for an $a_0 = 18$ laser colliding with a $\langle\gamma\rangle = 5860$ beam.

Fig. 5(a) was generated using a monoenergetic, collimated beam, however a finite energy spread and divergence will affect the measurement. Indeed, in Fig. 5(b) we see that divergence and energy spread result in fewer photons existing above the classical edge. For energy spreads $\sigma_\gamma > 20\%$ and divergence angles > 3 mrad, almost no photons exist above the edge. Without taking into account how these photons would be detected, this therefore already places a limit experimentally on the necessary beam properties.

C. keV photon LMA vs. LCFA angles

The final signature that we will consider is the lower edge of the angular emission for LMA and LCFA. In section III A we considered the separation between the harmonics as a signture to differentiate between LMA and LCFA, however, the angle of emission that LCFA predicts also appear over a larger range of scattering angles at a particular energy. In Fig. 1, in the keV range LCFA predicts photons scattered to angles closer to the axis of propagation. If we consider only photons will energies

< 10 keV being detected on a CCD, LMA will predict an on=axis hole in the spatial profile of the photons while LCFA predicts photons covering the detector, however the maximum of the spatial profile does not necessarily occur on-axis. While this signature then seems very promising from a measurement perspective, it is actually made very difficult by other sources of radiation. In particular, betatron radiation will appear on-axis and fill in the x-ray spatial profile. Therefore, experimentally the spatial profile will appear to be similar to that of LCFA regardless of whether it is actually correct. The best signature that may allow us to validate the LCFA and LMA is therefore the harmonics as we previously described.

IV. CONCLUSIONS

ACKNOWLEDGEMENTS

This work was supported by the National Science Foundation and Czech Science Foundation under NSF-GACR collaborative grant 2206059 and NSF grant 2108075. SSB was supported by U.S. Department of Energy Office of Science Offices of High Energy Physics and Fusion Energy Sciences (through LaserNetUS), under Contract No. DE-AC02-05CH11231.

AUTHOR DECLARATIONS

Conflict of Interest

The authors have no conflicts to disclose.

Author Contributions

Brandon K. Russell: **Stepan S. Bulanov**: **Qian Qian**: **Sergei V. Bulanov**: **Gabriele M. Grittani**: **Daniel Seipt**: **Christiopher Arran**: **Christopher P. Ridgers**: **Thomas Blackburn**: **Stuart P. D. Mangles**: **Alexander G. R. Thomas**:.

DATA AVAILABILITY

The data that support the findings of this study are available from the corresponding author upon reasonable request.

REFERENCES

[1]T. G. Blackburn, B. King, and S. Tang, "Simulations of laser-driven strong-field qed with ptarmigan: Resolving wavelength-scale interference and γ-ray polarization," (2023), arXiv:2305.13061 [hep-ph].

[2]D. Seipt, T. Heinzl, M. Marklund, and S. S. Bulanov, "Depletion of intense fields," Phys. Rev. Lett. **118**, 154803 (2017).

[3]F. Albert, B. B. Pollock, J. L. Shaw, K. A. Marsh, J. E. Ralph, Y.-H. Chen, D. Alessi, A. Pak, C. E. Clayton, S. H. Glenzer, and C. Joshi, "Angular dependence of betatron x-ray spectra from a laser-wakefield accelerator," Phys. Rev. Lett. **111**, 235004 (2013).

[4]K. Behm, A. Hussein, T. Zhao, R. Baggott, J. Cole, E. Hill, K. Krushelnick, A. Maksimchuk, J. Nees, S. Rose, A. Thomas, R. Watt, J. Wood, V. Yanovsky, and S. Mangles, "Demonstration of femtosecond broadband x-rays from laser wakefield acceleration as a source for pump-probe x-ray absorption studies," High Energy Density Physics **35**, 100729 (2020).

[5]J. M. Cole, K. T. Behm, E. Gerstmayr, T. G. Blackburn, J. C. Wood, C. D. Baird, M. J. Duff, C. Harvey, A. Ilderton, A. S. Joglekar, K. Krushelnick, S. Kuschel, M. Marklund, P. McKenna, C. D. Murphy, K. Poder, C. P. Ridgers, G. M. Samarin, G. Sarri, D. R. Symes, A. G. R. Thomas, J. Warwick, M. Zepf, Z. Najmudin, and S. P. D. Mangles, "Experimental evidence of radiation reaction in the collision of a high-intensity laser pulse with a laser-wakefield accelerated electron beam," Phys. Rev. X **8**, 011020 (2018).

[6]K. T. Behm, J. M. Cole, A. S. Joglekar, E. Gerstmayr, J. C. Wood, C. D. Baird, T. G. Blackburn, M. Duff, C. Harvey, A. Ilderton, S. Kuschel, S. P. D. Mangles, M. Marklund, P. McKenna, C. D. Murphy, Z. Najmudin, K. Poder, C. P. Ridgers, G. Sarri, G. M. Samarin, D. Symes, J. Warwick, M. Zepf, K. Krushelnick, and A. G. R. Thomas, "A spectrometer for ultrashort gamma-ray pulses with photon energies greater than 10 MeV," Review of Scientific Instruments **89** (2018), 10.1063/1.5056248, 113303, https://pubs.aip.org/aip/rsi/article-pdf/doi/10.1063/1.5056248/14703752/113303_1_online.pdf.